1941 nm Q-switched thulium-doped fiber laser with a multi-layer black phosphorus saturable absorber

A. A. LATIFF[a], M. F. M. RUSDI[b], Z. JUSOH[c], M. YASIN[d], H. AHMAD[a], S. W. HARUN[a,b,*]
[a]Photonics Research Centre, University of Malaya, 50603 Kuala Lumpur, Malaysia
[b]Department of Electrical Engineering, University of Malaya, 50603 Kuala Lumpur, Malaysia
[c]Faculty of Electrical Engineering, Universiti Teknologi Mara (Terengganu), 23000 Dungun, Terengganu, Malaysia
[d]Department of Physics, Faculty of Science and Technology, Airlangga University, Surabaya (60115) Indonesia

We demonstrate a Q-switched Thulium-doped fiber laser (TDFL) operating at 1941 nm region based on multi-layer black phosphorous (BP) as a saturable absorber (SA). The BP-based SA was prepared by mechanically exfoliating BP crystal and fixing the acquired BP flakes onto the scotch tape. A small piece of the tape was then sandwiched between two ferrules and incorporated in TDFL cavity to achieve stable Q-switched operation in conjunction with 1552 nm core pumping. The pulse repetition rate of the laser could be varied from 15.32 to 27.82 kHz, by tuning the pump power from 495 to 645 mW. At 645 mW pump power, the laser showed the average output power, pulse energy, and pulse width of 14 mW, 0.50 μJ, and 4.38 μs, respectively. Our results show that multi-layer BP is a promising SA for Q-switching laser operation in 2-micron region.

1. Introduction

Passively Q-switched fiber lasers have attracted much attention in recent years due to their potential applications in micromachining, metrology, medicine, telecommunications and fiber optical sensing [1, 2]. Compared with the active technique, the passive Q-switching technique based on saturable absorbers (SAs) has significant advantages in compactness, simplicity, and flexibility of implementation [1]. To date, various SAs have been implemented, such as nonlinear polarization rotation (NPR) [3], semiconductor saturable absorber mirrors (SESAMs) [4], carbon nanotubes (CNTs) [5] and 2D materials including, graphene [6], topological insulators (TIs)[7], and transition metal dichalcogenides (TMDs)[8]. However, due to certain intrinsic drawbacks of these SAs, such as environmental sensitivity, complex optical alignments, complicated fabrication and expensive packaging, or limited operating bandwidth, their optical applications are restricted. Therefore, there is constantly a strong motivation to seek new high-performance SAs for pulsed laser systems.

These days, black phosphorus (BP), a newly emerged 2D material, has also gained wide attention for potential application in developing the next-generation optoelectronics devices such as a sensor, field-effect transistors and solar cells [9, 10]. Stimulated by the similarity between graphene and BP in terms of single elemental component and direct band-gap, it is natural to find out whether BP could be used as an SA for the Q-switching and mode-locking applications [11]. Compared

to other 2D materials, the BP band-gap is depended on its layer number [12]. The electron mobility for each layer of BP will change from 0.3 eV (Bulk) to 2.0 eV (single-layer). This characteristic can be used to replenish the band-gap between semi-metallic graphene and TMDs materials. BP also has a promising broadband nonlinear optical response within infrared and mid-infrared regions [13]. Recently, Jiang et al. demonstrated the 1935 nm Q-switched fiber laser by using a powder BP as a passive Q-switcher [14]. This Q-switched fiber laser utilizes a Thulium-Holmium doped fiber (THDF) as a gain medium, and generate a pulse energy of 0.1 μJ. In this paper, we report what we believe to be among the highest pulse energy demonstration of a passively Q-switched Thulium-doped fiber laser (TDFL) operating at 1941 nm wavelength with a simple preparation of multi-layer BP as an SA. Note that BP comprises only the elemental "phosphorus". Hence, it could be easily peeled off by mechanical exfoliation.

2. Preparation and characterization of the BP based SA

In this work, the BP based SA was prepared by mechanical exfoliation method, which has been widely used in graphene-based ultra-fast fiber laser applications [15]. Mechanical exfoliation is advantageous mainly because of its simplicity and reliability, where the entire fabrication process is free from complicated chemical procedures and costly instruments. As shown in Fig. 1,

relatively thin flakes were peeled off from a big block of commercially available BP crystal (purity of 99.995 %) using clear scotch tape. Then, we repeatedly pressed the flakes stuck on the scotch tape so that the BP flakes become thin enough to transmit light with high efficiency. We cut a small piece of the BP tape and attached it onto a standard FC/PC fiber ferrule end surface with index matching gel. After connecting it with another FC/PC fiber ferrule with a standard flange adapter, the all-fiber BP based SA was finally ready. Exposing to oxygen and water molecules in a long period may degrade the performance of SA, ever since BP materials are hydrophilic. Therefore, the whole preparation process was done very fast in less than a minute. Due to the hydrophilic characteristic, the exfoliated BP was not directly attached to the end of fiber ferrule without the scotch tape.
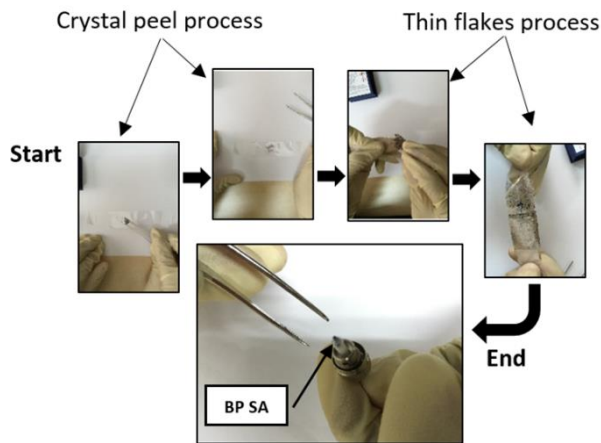
Fig. 1. The preparation flow of BP-SA using mechanical exfoliation method

We verify the quality of the BP tape by using Field Emission Scanning Electron Microscopy (FESEM) as shown in Fig. 2(a). The FESEM image shows the existence of the uniform layers and confirms the absence of > 1µm aggregates or voids in the composite SA, which otherwise result in non-saturable scattering losses. The composition of the transferred layers is confirmed by the Energy Dispersive Spectroscopy (EDS) on the FESEM image. The presence of BP material on the scotch tape adhesive surface was confirmed by the presence of higher peak phosphorus in the spectroscopy data as shown in Fig. 2(b). We also performed Raman spectroscopy on the fabricated BP tape sample. Fig. 2(c) shows the Raman spectrum, which is recorded by a spectrometer when a 514 nm beam of an Argon ion laser is radiated on the tape for 10 ms with an exposure power of 50 mW. As shown in the figure, the sample exhibits three distinct Raman peaks at 360 cm^{-1}, 438 cm^{-1} and 465 cm^{-1} [16], corresponding to the A_g^1, B_{2g} and A_g^2 vibration modes of layered BP. While the B_{2g} and A_g^2 modes correspond to the in-plane oscillation of phosphorus atoms in BP layer, the A_g^1 mode corresponds to the out-of-plane vibration. The ratio between A_g^1 peak (0.2168) and silicon (Si) level at 520

cm^{-1}(0.1579) estimates the thickness of BP flake as ~ 8.88 nm [16]. The thickness for single-layer BP is about 0.53 nm [12], thus the prepared BP based SA is expected to consist of 17 layers.
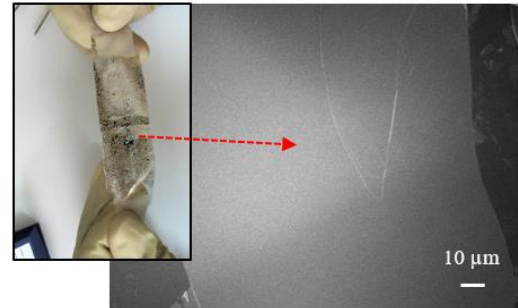
(a)
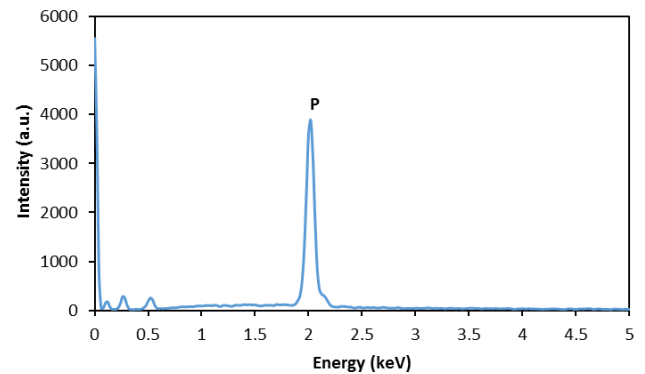
(b)
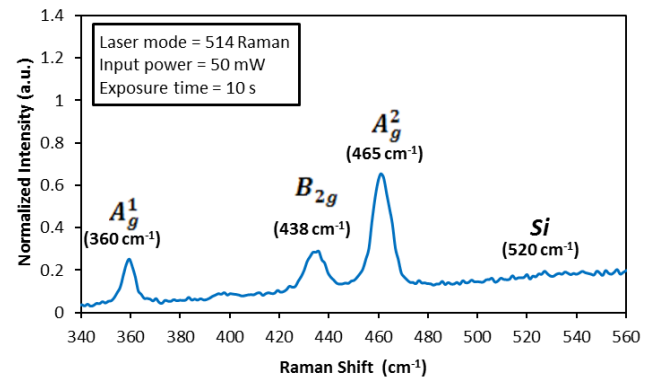
(c)

Fig. 2. Material characteristics of the BP based SA (a) FESAM image of the BP tape. The inset shows the BP layer on a scotch tape. (b) EDS data for confirming the presence of phosphorus. (c) Raman spectrum of the multi-layered BP tape

The nonlinear optical response property for the multilayer BP on the scotch tape was then investigated to confirm its saturable absorption by applying an absorption technique. A self-constructed mode-locked fiber laser (1557 nm wavelength, 1.5 ps pulse width, 17.4 MHz repetition rate) was used as the input pulse source. The

transmitted power and also a reference power for normalization were recorded as a function of incident intensity on the tape by varying the input laser power. With increasing peak intensity, the material absorption decreases as shown in Fig. 3, confirming saturable absorption. The experimental data for absorption are fitted according to $\alpha(I)=\alpha_s/(1+I/I_{sat})+\alpha_{ns}$ [17, 18]. $\alpha(I)$ is the absorption, α_s is the modulation depth, I is the input intensity, I_{sat} is the saturation intensity, and α_{ns} is the non-saturable absorption. As shown in Fig. 3, the modulation depth, non-saturable absorption, and saturation intensity are obtained to be 7 %, 58 % and 0.25 MW/cm^2, respectively. Taking into account its nonlinear optical response leading to absorption saturation at relatively low fluence, the mechanically exfoliated BP meets basic criteria of a passive SA for fiber lasers. Lu et al. reported the nonlinear saturable absorption profile using 1563 nm and 1930 nm mode-locked laser sources [13]. In their work, modulation depth at 2-micron region has ~ 3 % slightly lower than 1.55-micron region. Similar work has been done by Sotor et al. by showing the modulation depth of 4.1% using 1560 nm mode-locked laser [19]. They manage to generate ultrafast laser at 1910 nm. In our work, the obtained modulation depth is about 7% by using 1557 mode-locked laser. This shows our BP tape modulation depth is higher and promising to work as an SA at 2-micron region.
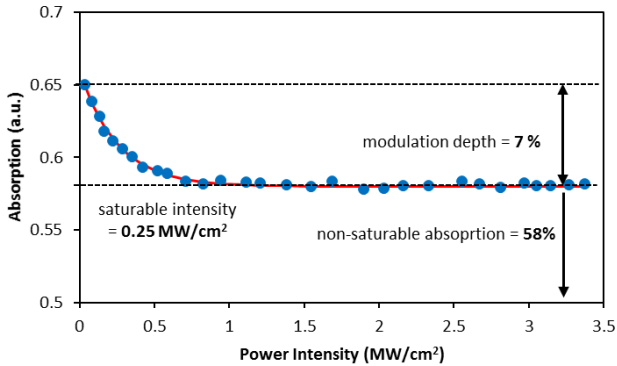
Fig. 3. Nonlinear saturable absorption profile showing saturable absorption

3. Experimental setup

The experimental setup of our proposed passively Q-switched TDFL is schematically shown in Fig. 4. It uses a 5 m long Thulium-doped fiber (TDF, Nufern) as a gain medium , which was core-pumped by a home-made 1552 nm Erbium-Ytterbium doped fiber laser (EYDFL) pump via a 1550/2000 nm wavelength division multiplexer (WDM). The TDF used has a numerical aperture of 0.15, loss of less than 0.2 dB/km at 1900 nm, and peak core absorptions at 1180 and 793 nm are 9 and 27 dB/m, respectively. The multilayer BP on the scotch tape acted as a passive Q-switcher. It was integrated into the fiber laser cavity by sandwiching a ~1 mm × 1 mm piece of the

composite tape between two fiber connectors, adhered with index matching gel. It has to note that the BP-SA is polarization-dependent due to anisotropic layered material characteristic [12]. So the polarization controller (PC) is employed to adjust the coupling of light from the fiber to the absorber. The signal was coupled out using 10 dB output coupler which keeps 90% of the light oscillating unidirectional in the ring cavity for both spectral and temporal diagnostics. Then, stable lasing was generated without implementing polarization independent isolator. This also contributes to reducing cavity loss. The laser output from the coupler was simultaneously monitored using a 500-MHz oscilloscope (OSC, WAVEJET) together with a 7-GHz photodetector (PD, EOT), a 7.8 GHz radio-frequency (RF, Anritsu) spectrum analyzer and an optical spectrum analyzer (OSA, Yokogawa) with a spectral resolution of 0.05 nm. The cavity length of the ring resonator is measured to be around 13.5 m.
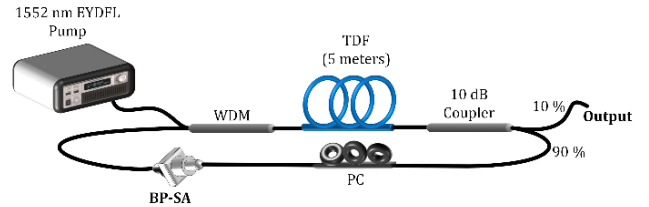
Fig. 4. Experimental setup of the proposed Q-switched TDFL employing a multi-layered BP on the scotch tape

4. Results and discussion

In the experiment, the Q-switched laser is self-started as the pump power is increased just above the threshold pump power of 495 mW. The stable Q-switched laser operation is maintained as the pump power increased to 645 mW, then unstable up to 715 mW before it disappears. Fig. 5 shows typical oscilloscope traces of the Q-switched pulse trains at pump powers of 495 mW, 503 mW, 645 mW and 716 mW. Unlike the fixed repetition rate of a mode-locked fiber laser, the pulse repetition rate in our laser increased with the pump power from 15.32 to 30.86 kHz, which is a typical feature of passive Q-switching operation [3]. Meanwhile, the pulse width is narrowed from 4.56 to 2.92 μs as the pump power increased from 495 to 716 mW. To verify that the passive Q-switching was attributed to the SA, the BP tape is removed from the cavity. In this case, no Q-switched pulses are observed on the oscilloscope even when the pump power was adjusted over a wide range. This finding has confirmed that the BP-based SA is responsible for the passively Q-switched operation of the laser. Another observation is an SA threshold damage. So far at 716 mW pump power and beyond, the BP-SA can still operate normally without any degradation of laser performance or damage.
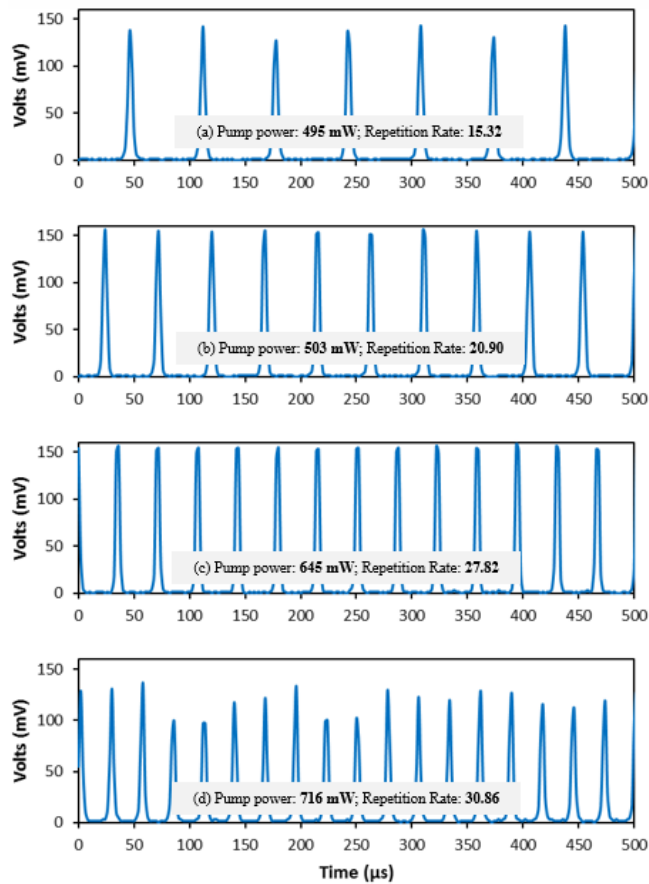
Fig. 5. Typical oscilloscope trace of the Q-switched TDFL as the pump power is varied from (a) 495 mW, (b) 503 mW, (c) 645 mW, and 716 mW

Fig. 6. Output spectrum of the Q-switched TDFL at a 1552 nm pump power of 590 mW

The output optical spectral of the Q-switched pulses emitted from the fiber laser at a pump power of 590 mW are presented in Fig. 6. The laser emission spectrum has low multiple peaks with a center wavelength of 1941 nm corresponding to nonlinear polarization rotation (NPR) effect. When the TDF is pumped by a 1552 nm EYDFL to generate population inversion of Thulium ions, an amplified spontaneous emission (ASE) is produced in around 1.9 µm region via spontaneous and stimulated emission processes. The ASE oscillates in the ring cavity to generate laser when the gain overcomes the total cavity loss. With increasing power of the pump, the multi-wavelength laser is generated due to the effect of the TDF birefringence, which induced phase variation in the ring laser cavity based on NPR effect. The NPR can induce intensity-dependent loss (IDL) to alleviate mode competition caused by a homogeneous broadening in the gain medium. Since the TDF used in the cavity has a reasonably high nonlinearity, it produces sufficient NPR- and four-wave mixing (FWM)-induced IDL effect in the laser cavity. In this case, the transmission term varies too fast with the power and thus allows multiple wavelengths to oscillate in the ring cavity.

In order to study the stability of Q-switched laser pulses, we also measured the radio frequency (RF) spectrum of the TDFL at various pump powers as shown in Fig. 7. Based on Fourier transform, these RF patterns are corresponded to its time domain (Fig. 5). The signal-to-noise ratios are obtained at 18.0, 24.1, 31.8 and 27.2 dB at pump powers of 495, 503, 645 and 716 mW, respectively. This shows that the stability of passively Q-switched state is highest at a pump power of 645 mW, which provides the repetition rate of 27.8 kHz with the pulse width of 4.38 µs. Stability of the BP Q-switched fiber laser is also monitored over a time span of 4 hours; the average output power of the laser is kept in a consistent value with little fluctuations. Before the Q-switched state disappears above pump power of 716 mW, the highest repetition rate of 30.86 kHz with the lowest pulse width is obtained. However the Q-switched state is unstable. In addition, we also measured the average output power and correspondingly calculated the single-pulse energy. Throughout the experiment, we can confirm that no mode-beating frequency was present.

Fig. 8 plots the measured average output power and correspondingly calculate the single-pulse energy. The average output power almost linearly increased with the input pump power and at the 1552 nm pump power of 645 mW, the maximum average output power of stable Q-switched state is 14 mW. The slope efficiency of the Q-switched laser is calculated to be around 7.32 %. One can see from the figure that the pulse energy also increases with the pump power. The maximum pulse energy is 0.50 µJ. We believe that the performance of Q-switched pulses produced by the laser could be further improved by optimizing the SA parameters of BP tape and the cavity design. We also tried to get the BP mode-locked TDFL operation with a much longer cavity by adding 100 - 200 m single mode fiber to increase the pulse energy of the cavity mode random surge of the background noise. A strong pulse train with a pulse period equal to the cavity round trip time could be clearly observed but was difficult to be stabilized. We think the high cavity loss is the main reason for preventing the laser from the stable mode-locking operation, but both the cavity and BP based SA are needed to be further optimized, such as cavity length,

cavity loss, cavity polarization and modulation depth of the SA, etc. A future work will focus on shortening cavity length by adopting a short linear cavity as well as reducing the number of BP layers of the SA.
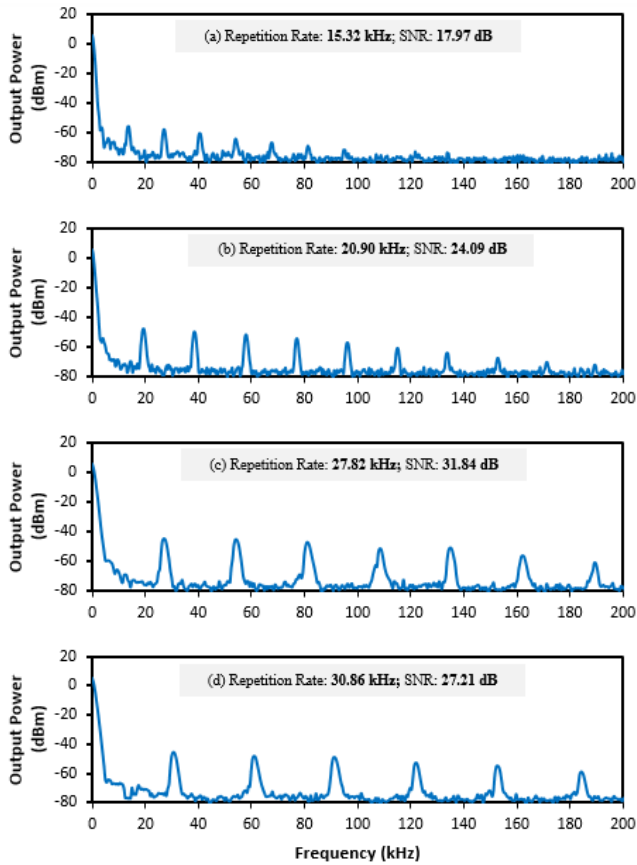
Fig. 7. RF spectrum of the Q-switched TDFL at various 1552 nm pump power (a) 495 mW (b) 503 mW (c) 645 mW and (d) 716 mW
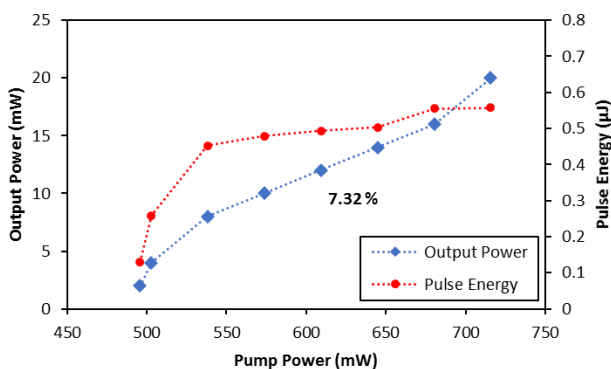
Fig. 8. Output power and calculated pulse energy within 495 to 715 mW pump power

5. Conclusion

We experimentally demonstrated a passively Q-switched ring TDFL using a multi-layer BP flakes onto a scotch tape as an SA. The tape with ~ 17 layers of BP was prepared by the mechanical exfoliation method and sandwiched between two FCs with a fiber adapter to form a fiber-compatible BP-based SA. Stable Q-switched pulse train at 1941 nm region was successfully obtained within the 1552 nm pump power range from 495 mW to 645 mW. At the maximum pump power, the laser showed the average output power, high pulse energy, and pulse width of 14 mW, 0.50 μJ, and 4.38 μs, respectively. The pulse repetition rate could be varied over a wide range of frequencies, from 15.32 to 27.82 kHz, by tuning the pump power. Our experimental results suggest that multi-layer BP is a promising material for pulsed laser applications.

Acknowledgements

References

[1] M. C. Pierce, S. D. Jackson, P. S. Golding, B. Dickinson, M. R. Dickinson, T. A. King, P. Sloan, BiOS 2001 The International Symposium on Biomedical Optics, International Society for Optics and Photonics 144 (2001).

[2] D. Creeden, P. A. Budni, P. A. Ketteridge, SPIE LASE: Lasers and Applications in Science and Engineering, International Society for Optics and Photonics 71950X-71950X-71955 (2009).

[3] S. Azooz, S. W. Harun, H. Ahmad, A. Halder, M. C. Paul, S. Das, S. K. Bhadra, Ukrainian Journal of Physical Optics **16**, 32 (2015).

[4] M. A. Chernysheva, A. A. Krylov, N. R. Arutyunyan, A. S. Pozharov, E. D. Obraztsova, E. M. Dianov, Selected Topics in Quantum Electronics, IEEE Journal of **20**, 448 (2014).

[5] A. Martinez, Z. Sun, Nature Photonics **7**, 842 (2013).

[6] N. Saidin, D. Zen, B.A. Hamida, S. Khan, H. Ahmad, K. Dimyati, S. W. Harun, Laser Physics **23**, 115102 (2013).

[7] J. Lee, M. Jung, J. Koo, C. Chi, J. H. Lee, Selected Topics in Quantum Electronics, IEEE Journal of **21**, 31 (2015).

[8] Z. Tian, K. Wu, L. Kong, N. Yang, Y. Wang, R. Chen, W. Hu, J. Xu, Y. Tang, Laser Physics Letters **12**, 065104 (2015).

[9] L. Li, Y. Yu, G. J. Ye, Q. Ge, X. Ou, H. Wu, D. Feng, X. H. Chen, Y. Zhang, Nature Nanotechnology **9**, 372 (2014).

[10] M. Buscema, D. J. Groenendijk, G. A. Steele, H. S. J. van der Zant, A. Castellanos-Gomez, Nature Communications 5 (2014).

[11] Y. Chen, G. Jiang, S. Chen, Z. Guo, X. Yu, C. Zhao, H. Zhang, Q. Bao, S. Wen, D. Tang, Optics Express **23**, 12823 (2015).

[12] F. Xia, H. Wang, Y. Jia, Nature Communications 5 (2014).

[13] S. Lu, L. Miao, Z. Guo, X. Qi, C. Zhao, H. Zhang, S. Wen, D. Tang, D. Fan, Optics Express **23**, 11183 (2015).

[14] T. Jiang, K. Yin, X. Zheng, H. Yu, X.-A. Cheng, arXiv preprint arXiv:1504.07341, (2015).

[15] K. S. Novoselov, V. Fal, L. Colombo, P. Gellert, M. Schwab, K. Kim, Nature **490**, 192 (2012).

[16] A. Castellanos-Gomez, L. Vicarelli, E. Prada, J. O. Island, K. Narasimha-Acharya, S. I. Blanter, D. J. Groenendijk, M. Buscema, G. A. Steele, J. Alvarez, 2D Materials **1**, 025001 (2014).

[17] H. Mu, S. Lin, Z. Wang, S. Xiao, P. Li, Y. Chen, H. Zhang, H. Bao, S. P. Lau, C. Pan, Advanced Optical Materials **3**, 1447 (2015).

[18] E. Garmire, Selected Topics in Quantum Electronics, IEEE Journal of **6**, 1094 (2000).

[19] J. Sotor, G. Sobon, M. Kowalczyk, W. Macherzynski, P. Paletko, K. M. Abramski, Optics Letters **40**, 3885 (2015).

_____
[*]Corresponding author: swharun@um.edu.my